Lyapunov Based PI Controller for PEM Fuel Cell Based Boost Converter

Ilhan Kocaarslan*, Sude Kart**, Yener Altun***, Naci GENC****

*Department of Electrical Engineering, Istanbul University, Istanbul, Turkey

** Department of Electrical Electronics Engineering, Hakkari University, Hakkari, Turkey

*** Department of Business Administration Faculty of Management, Van Yuzuncu Yil University, Van, Turkey

**** Department of Electrical Electronics Engineering, Faculty of Engineering, Van Yuzuncu Yil University, Van, Turkey

(ilhankocaarslan@gmail.com, sudecavus@gmail.com, yeneraltun@yyu.edu.tr, nacigenc@yyu.edu.tr)

‡ Corresponding Author; Naci Genc, Faculty of Engineering, Van Yuzuncu Yil University, 65080, Turkey,

Tel: +90 555 418 0321, nacigenc@yyu.edu.tr

Received: 29.01.2020 Accepted:29.02.2020

Abstract- Proton Exchange Membrane Fuel Cell (PEMFC) which is an efficient renewable energy system has usage area in home and industrial applications. Since the generated voltage from PEMFC is low, the output voltage of it can be increased by using a boost converter. The boost converter fed by PEMFC can normally be controlled by the classical PI controller which parameters (K_P, K_i) are constant and do not depend on the circuit parameters. Therefore, these coefficients are non-adaptive at variable load situations. In this study, an improved controller is obtained by regulating the PI controller according to Lyapunov stability theorem. Then, this improved Lyapunov based PI controller is proposed for PEMFC based boost converter. In the proposed method, K_P and K_i parameters vary adaptively depending on the circuit parameters. Thus, the system works more stable and settling time of system's output voltage signal decreased compared to classical PI controller. The proposed method has been successfully tested in Matlab/Simulink environment.

Keywords PEMFC; Boost converter; PI controller; Lyapunov stability.

1. Introduction

The need for clean energy in the world is increasing and accordingly studies on renewable energy sources are accelerating. Some of the renewable energy sources are biomass, geothermal, fuel cell, solar and wind energy. Solar energy is at the center of renewable energy sources. Solar energy is the main source of many renewable energies [1]. Among these, most of the studies are concentrated on fuel cell. Fuel cell which is an electrochemical device that converts hydrogen fuel to electricity without burning process has many good features such as high efficiency, fast response, modular production [2]. It is playing an important role as renewable energy source for energy generation in portable systems [3]. Among fuel cell technologies, Proton Exchange Membrane (PEM) fuel cells are ideal options for home and office applications in terms of energy production at relatively low operating temperatures and high efficiency. The operation of the proton exchange membrane fuel cell is based on thermodynamic, hydrodynamic and mass transfer theories.

Performance of PEM fuel cell is defined with current and voltage characteristics of fuel cell. The current supplied by the PEM fuel cell is proportional to the amount of hydrogen consumed. As the voltage of the fuel cell decreases, the electricity produced per unit of hydrogen decreases. That means, the fuel cell voltage is considered to be a measure of the efficiency of the fuel cell [4]. In addition, since the output voltage of the fuel cell is low, its output voltage is boosted by DC-DC converter circuits for power generation in industrial applications [5].

DC-DC converters are non-linear systems. Therefore, it is important to design a controller. Generally, the preferred PI controller is a combined form of proportional and integral control. Proportional control generates the controller output based on error quantity and Kp coefficient. It increases the dynamic accuracy and dynamic response of the system. It is directly related to error and proportional control coefficient. The integral control adjusts the output of the controller according to the coefficient Ki and the amount of error. It increases static accuracy rather than dynamic response. Integral is a function of the control coefficient. The design principle of the PI controllers is based on the linearized small signal model around the operational point of the system.

Conventional control methods like PI controller are designed for nominal operating conditions, so they cannot show stability under different operating conditions. Therefore, the stability is important for classical PI controller [6-7]. When designing a controller for DC-DC converters, this linearization leads to the neglect of bilinear terms as the main source of non-linearity of the system. Therefore, these designs are not suitable for larger distortions such as large load variations. Because the stability and performance of the system cannot be analyzed for the first points away from the stationary operating point, Salimi [8] presented a new approach to closed loop control using Lyapunov based nonlinear controller. Despite a wide range of irradiation levels and temperature changes, the controller stabilizes the PV system at its maximum power point. Rezkallah et al. [9] applied a sliding mode control approach for the solar-PV grid interface system and applied Lyapunov equations to the stability of the system. Vatani et al. [10] examined Lyapunov stability of a DC-DC power converter controlled by a PI controller. They calculated the Lyapunov function using the sum of square programming method. Fahad et al. [11] designed a fractional-order (FO) controller for a grid-connected PV system and verified the stability of the system using the Lyapunov candidate function.

In this study, a Lyapunov based PI controller is improved and proposed for PEMFC based boost converter. It is aimed to ensure the stability of the PI controller when controlling the output voltage of the system. Moreover, controller coefficients (K_P, K_i) changes according to circuit parameters. For this purpose, the Lyapunov stability equations are applied to the boost equations for the derivative of the control signal of the output voltage goes to zero. In the study, the PEMFC was modelled and simulated in Matlab/Simulink environment to obtain the current-voltage and current-power characteristics of the PEMFC. Then, the designed PEMFC was connected to a DC-DC boost converter and the proposed improved control method was applied to the system.

2. Modeling and Analysis of the System

2.1. PEMFC Model

Since the operation of fuel cell systems is complex, it is important to model of a PEMFC for the better performance [12]. PEMFC was modelled and simulated in Matlab/Simulink environment to obtain the current-voltage and current-power characteristics. This model is simulated for different current densities and the graphs of the relationships between voltage, current, power and efficiency are shown in Figure 1 [13].

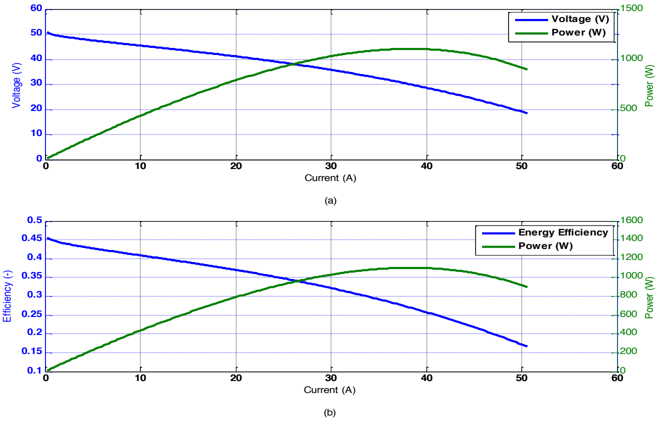

Fig. 1. a) I-V and I-P curves of PEMFC, (b) I- efficiency and I-P curves of PEMFC.

The maximum voltage produced by a cell that can be recycled is called reversible cell voltage. Reversible cell voltage can be calculated by using a type of Nernst equation [14] as shown in equation (1);

$$V_{rev} = 1.229 - 8.5\times10^{-4}\left(T_{FC} - 298.25\right) + 4.3085\times10^{-5}\times T_{FC}\left[\ln\left(P_{H_2}\right) + \frac{1}{2}\ln\left(P_{O_2}\right)\right] \quad (1)$$

The partial pressures of hydrogen and oxygen can be calculated as in equation (2) and equation (3), respectively;

$$P_{H_2} = \frac{1 - x_{H_2O,A}}{1 + (x_A/2)(1 + \xi_A/(\xi_A - 1))} P_A \quad (2)$$

$$P_{O_2} = \frac{1 - x_{H_2O,C}}{1 + (x_C/2)(1 + \xi_C/(\xi_C - 1))} P_C \quad (3)$$

The operating cell voltage is less than reversible cell voltage due to irreversibility and over-potential. The operating cell voltage can be expressed as;

$$V_{operating} = V_{rev} - V_{irrev} \quad (4)$$

Activation losses, ohmic losses, mass transport, or concentration losses are the over-potentials considered here.

$$V_{irrev} = V_{act} + V_{ohm} + V_{con} \quad (5)$$

After the irreversibility is calculated, the power generated by the stack is calculated by equation (6).

$$W_{stack} = V_{operating} . i . A_{cell} . n_{cell} \quad (6)$$

Here, n_{cell} is the number of fuel cells in the stack. A_{cell} is the area of each cell and i is the current density [15].

2.2. The DC-DC Boost Converter

The DC-DC boost converter which design considerations and modeling equations are studied in the literature [16-18] consists of one active switch (*S*); *L* inductor for boosting; D_o diode; *C* capacitor. A boost converter circuit using a power MOSFET is shown in Figure 2. In a boost converter the average output voltage V_0 is higher than the source voltage V_{FC}.

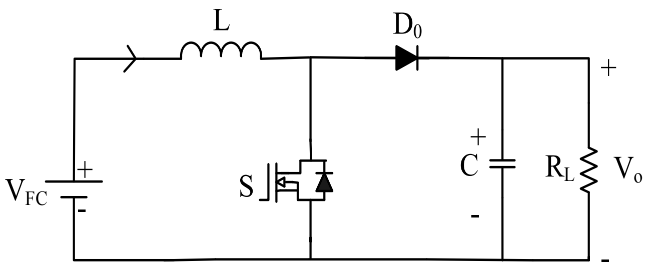

Fig. 2. DC/DC Boost converter.

The relationship between the duty cycle and the output voltage is given in Eq. (7).

$$\frac{V_o}{V_{FC}} = \frac{1}{(1-D)} \tag{7}$$

State-space-average model is a technique for creating a time-invariant model [19]. It is important to perform the state space average model and small signal analysis to find the transfer function of the system. State space average model is found with the help of equation (8).

$$\begin{bmatrix} \frac{di_L}{dt} \\ \frac{dV_o}{dt} \end{bmatrix} = \begin{bmatrix} 0 & -\frac{(1-D)}{C} \\ \frac{(1-D)}{C} & -\frac{1}{R_L C} \end{bmatrix} \begin{bmatrix} i_L \\ V_o \end{bmatrix} + \begin{bmatrix} \frac{1}{L} \\ 0 \end{bmatrix} [V_{FC}] \tag{8}$$

This equation can be expressed as follows.

$$\begin{bmatrix} \dot{x}_1 \\ \dot{x}_2 \end{bmatrix} = \begin{bmatrix} 0 & -\frac{(1-D)}{C} \\ \frac{(1-D)}{C} & -\frac{1}{R_L C} \end{bmatrix} \begin{bmatrix} i_L \\ V_o \end{bmatrix} + \begin{bmatrix} x_1 \\ x_2 \end{bmatrix} [V_{FC}] \tag{9}$$

where;

D: Duty cycle

V_{FC}: input voltage

V_o: Capacitor Voltage, DC output voltage

R_L: Load resistance

i_L: Inductance Current

3. Result Design of the Proposed Controlled

In the classical PI controller (Figure 3), the difference between the reference and the actual value (*e*) is regulated by the controller to obtain the *k* control signal. The resulting *k* control signal should be constant at steady state. Therefore, the derivative of the control signal *k* must be equal to zero at steady state. Lyapunov equations was applied by using this feature of the controller output signal at the steady state to improve the proposed controller.

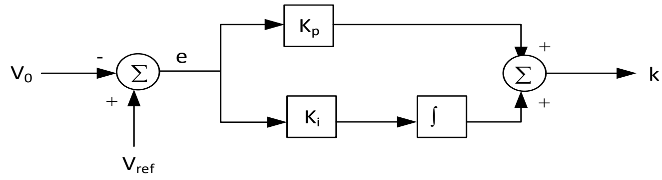

Fig. 3. The classical PI controller.

The output signal of the PI controller (*k*) should be constant at steady state as given in equation 10.

$$z = \frac{dk}{dt} = 0 \tag{10}$$

For the proposed controller to be designed, *z* must be defined as follows. Where V^* is defined as reference output voltage.

$$z = \frac{dk}{dt} = 0 = \frac{d}{dt}\left[\left(V^* - x_2\right)K_P + K_I \int \left(V^* - x_2\right)dt\right] \tag{11}$$

If the equation 11 is combined with equation 9, the equation 12 can be obtained.

$$z = K_P \frac{1-D}{C} x_1 - \frac{1}{R_L C} x_2 K_P - K_I \left(V^* - x_2\right) \tag{12}$$

The dynamics of the output signal according to system parameters can be shown as follows.

$$\dot{z} = K_P \frac{1-D}{C} \dot{x}_1 - K_P \frac{\dot{D}}{C} x_1 - \frac{1}{R_L C} K_P \dot{x}_2 + K_I \dot{x}_2$$

(13)

Combining equations 9 and 13, equation 14 is obtained.

$$\dot{z} = K_P \frac{1-D}{C}\left[-\left(\frac{1-D}{L}\right)x_2 + \frac{V_{FC}}{L}\right] - K_P \frac{\dot{D}}{C} x_1 - \left(\frac{1-D}{C} x_1 - \frac{1}{R_L C} x_2\right)\left(\frac{1}{R_L C} K_P - K_I\right) \tag{14}$$

The equations 12 and 14 can be improved by using the Lyapunov function. The Lyapunov function of the system can be defined as given in equation 15 to improve the controller. Also, the derivative of the Lyapunov function can be given in equation 16 [8].

$$V = \frac{1}{2} z^2 \tag{15}$$

$$\dot{V} = z\dot{z} \tag{16}$$

If the error is assumed as $\dot{z} = -\lambda z$, the derivative of the Lyapunov function will be $\dot{V} = -\lambda z^2$. Since the scalar λ is a positive constant, the derivative of the Lyapunov function will be a negative semi-defined function. Thus, the asymptomatic stability of the system is guaranteed and the error variable of the system (*z*) is limited. Briefly, according to equations (12), (13) and $\dot{z} = -\lambda z$, the equation of the proposed Lyapunov based controller can be obtained as follow.

$$\dot{z}+\lambda z=K_P\frac{(1-D)}{C}\left[-\frac{(1-D)}{L}x_2+\frac{V_{FC}}{L}\right]$$
$$-K_P\frac{\dot{D}}{C}x_1-\left(\frac{1-D}{C}x_1-\frac{1}{R_LC}x_2\right)\left(\frac{1}{R_LC}K_P-K_I\right) \quad (17)$$
$$+\lambda\left[K_P\frac{(1-D)}{C}x_1-\frac{1}{R_LC}x_2K_P-K_I\left(V_o^*-x_2\right)\right]=0$$

By using the derivative of the Lyapunov function ($\dot{V}=-\lambda z^2$), the second derivative of the Lyapunov function will be $\ddot{V}=-2\lambda z\dot{z}$. According to Barbalat's lemma [17]; V must be a lower bounded function, $\dot{V}$ must be a negative semi-definite function and $\dot{V}$ must be a uniformly continuous function. Therefore, if these conditions are met, the error converges goes into zero in different operating conditions.

For a bounden variable of z, it is seen that the first and the second rules of the Barbalat's lemma are satisfied according to $\dot{V}=-\lambda z^2$. Also, it can be explained that the error variable and parameters of the model are bounded according to $\ddot{V}=-2\lambda z\dot{z}$ and the equation (13). In addition, since $\dot{V}$ is uniformly continuous function, the third condition is also satisfied. From this point, it is seen that the system has asymptotically stable behavior for a wide range of operation and the output error of the system goes to zero during steady state condition.

The duty cycle of the switching signal for the closed loop control of the boost converter can be calculated using equation (17). To describe the calculation approach more clearly, equation (17) can be re-written as equation (18). The equation (18) shows that the duty cycle is proportional of both controller coefficients and circuit parameters. This is the main contribution of the proposed controller and improves the dynamic behavior of the converter.

$$\dot{D}=\left[\frac{x_1K_P}{C}\right]^{-1}\left\{\begin{array}{l}\frac{(1-D)}{C}\left[-\frac{(1-D)}{L}x_2+\frac{V_o(1-D)}{L}-x_1\left(\frac{x_1(1-D)}{x_2C}K_P-K_I-\lambda K_P\right)\right]\\+\frac{x_1(1-D)}{C}\left(\frac{x_1(1-D)}{x_2C}K_P-K_I-\lambda K_P\right)-\lambda K_I\left(V_o^*-x_2\right)\end{array}\right\} \quad (18)$$

4. Simulation Results

The proposed Lyapunov based PI controller according to equation (18) is improved and proposed for PEMFC based boost converter as shown in Figure 4. Figure 5 shows the block diagram of the proposed controller. It is seen that the output voltage of the system changes according to controller coefficients (K_P, K_I) and circuit parameters. The parameters of the converter given in Table-1 are selected according to application. PEMFC with 1kW power rating is generally used in industrial and home applications with output voltage of 30-60V. The reference output voltage of the converter is selected as 200V which is used as dc input voltage for multilevel inverters. The circuit parameters were calculated according to design considerations [16-18]. Also the clasical Ziegler-Nichols method is used to calculate controller coefficients.

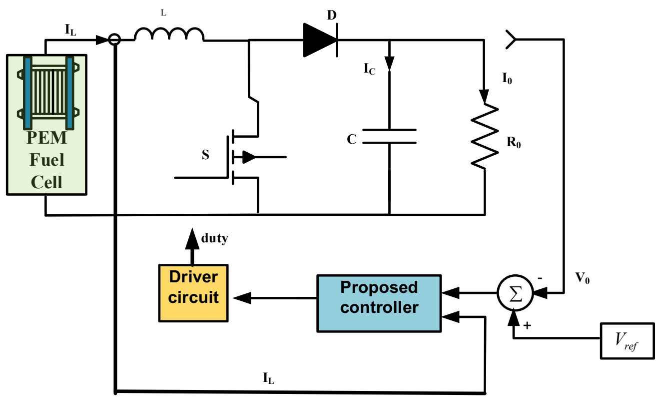

Fig. 4. The proposed Lyapunov based PI controller for PEMFC.

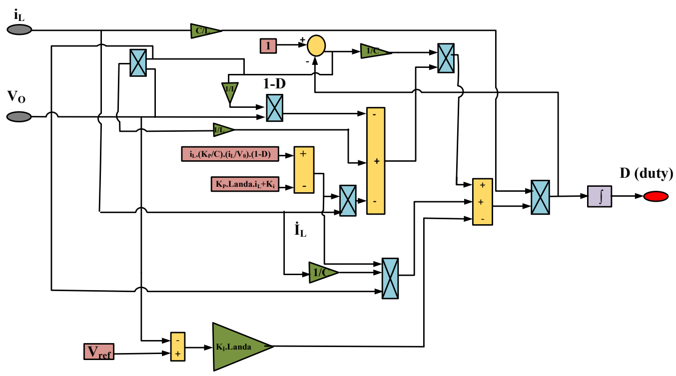

Fig. 5. The block diagram of the proposed controller.

Table 1. The parameters of the converter

PEMFC output voltage	30-60 V
Converter output voltage	200 V
Output power	1 kW
Inductance	100 µH
Capacitor	266 µF

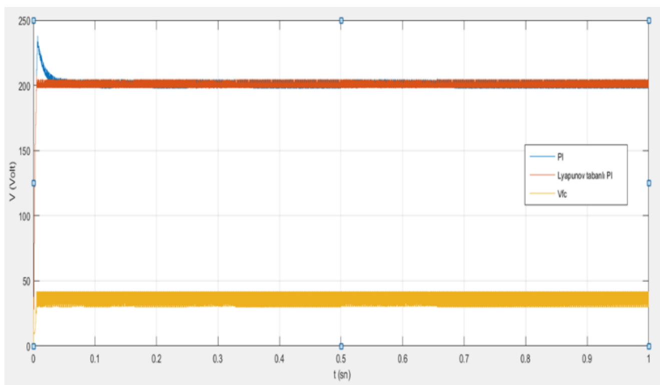

Fig. 6. Output voltage changes with respect to time (blue line: PI, red line: Lyapunov based PI, yellow line: output voltage of fuel cell).

Figure 6 shows a time-comparative graph of the output voltage of the system controlled by the classical PI controller and the Lyapunov-based PI controller. Also, the numerical comparison of the parameters in Figure 6 are given in Table 2.

Table 2. The numerical comparison of PI and proposed Lyapunov based controllers

Parameters	PI	Lyapunov based
Rising time	0.0068 sec	0.005 sec
Settling time	0.06 sec	0.005 sec
Overshoot	38 V (19%)	8 V
Ripple	6 V (3%)	6 V

According to Table 2, the rise time of Lyapunov-based PI controller is reduced by 26.4% compared to classical PI controller. The settling time of the signal was 91.6% faster than the classical PI controller and the overshoot of the proposed controller is 79.9% less than the classical PI controller.

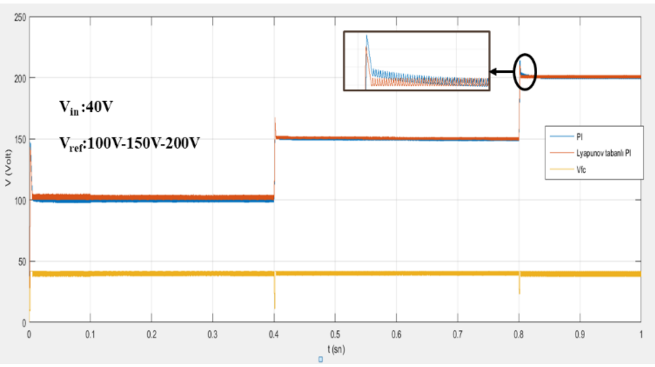

Fig. 7. Output voltage changes with respect to time for different (V_{ref}:100V-150V-200V) (blue line: PI, red line: Lyapunov based PI, yellow line: output voltage of fuel cell).

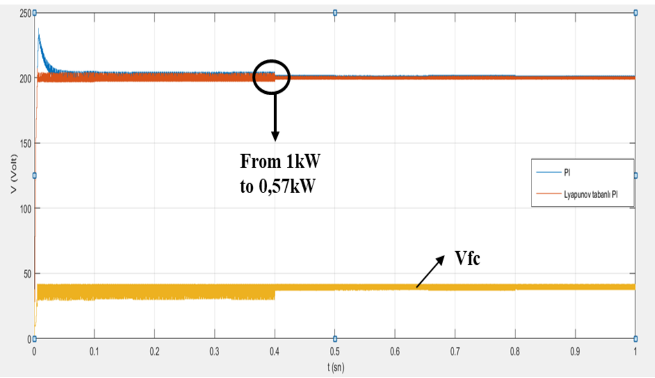

Fig. 8. The variation of the output voltage with respect to time under different loads. (RL: 40Ω-80Ω).

The proposed controller and classical PI controller have been tested under different dynamic conditions. First, PEMFC based converter is operated for different output voltage against constant input voltage. The input voltage of the converter (V_{FC}) was taken constant (40V) and output reference voltage was changed as 100V-150V-200V. Figure 7 shows the dynamic results of these difference reference voltages. Second, PEMFC based converter is operated under different loads for 200V output voltage (Figure 8). It is seen that the proposed Lyapunov-based PI controller performs reference tracking successfully under different dynamical conditions.

5. Conclusion

A Lyapunov based PI controller is improved and proposed for PEMFC based boost converter. Since the output voltage of a PEMFC is always changeable, it is needed to obtain a fixed output voltage via boost type DC-DC converter. Therefore, the output voltage controller is important for PEMFC. Due to the constant controller coefficients (K_P, K_i) of a classical PI controller the output voltage of the converter is affected under different dynamical changes. These coefficients are non-adaptive at variable load situations. However, in the proposed method PI controller is improved by using Lyapunov stability theorem. The output voltage is affected by controller coefficients and circuit parameters in the proposed controller. Therefore, the controller effect changes adaptively depending on the circuit parameters and load situations. Thus, the system works more stable and settling time of system's output voltage signal decreased compared to classical PI controller. The results show that better dynamical performances have been obtained with the proposed controller.

Acknowledgement

The authors would like to acknowledge Scientific and Technological Research Council of Turkey (TUBITAK) for the financial support of this research. This research is supported by the TUBITAK with project no: EEEAG-115E419.

References

[1] M. Karaca, N. Genc, A. Mamızadeh, A. Sular, “Analysis of Passive Filters for PV Inverters Under Variable Irradiances”, 8th International Conference on Renewable Energy Research and Applications (ICRERA), Braşov, Romania, pp. 680-685, 3-6 November, 2019.

[2] B. Zafar, “Design of a Renewable hybrid photovoltaicElectrolyze-PEM/Fuel Cell System using Hydrogen”, International Journal Of Smart Grid, vol.3, No. 4, pp. 201-207, 2019.

[3] L. Diaz-Saldiema, J. Leyva-Ramos, D. Langarica-Cordoba, J.A. Morales-Saldana, “Control strategy of switching regulators for fuel-cell power applications”, IET Renewable Power Generation. 11:799-805. DOI: 10.1049/iet-rpg.2016.0717.

[4] R. O’Hayre, S.W. Cha, W. Colella, , F.B Prinz, Fuel cell fundamentals, John Wiley& Sons, New Jersey, ISBN:0471741485, 2006.

[5] A. Sular, A. Mamızadeh, N. Genc, M. Karaca, “PV Power Based Duty Cycle Control of Quasi-Resonant Inverter for Induction Cooking”, 8th International Conference on Renewable Energy Research and

Applications (ICRERA), Braşov, Romania, pp. 804-809, 3-6 November, 2019.

[6] E. A. Mostafa and N.K. Bahgaat, "A Comparison Between Using A Firefly Algorithm and A Modified PSO Technique for Stability Analysis of a PV System Connected to Grid", International Journal of Smart Grid, vol.1, No. 1, pp. 1-8, 2017.

[7] T.K. Roy, M.A. Mahmud, "Active power control of three-phase grid-connected solar PV systems using a robust nonlinear adaptive backstepping approach", Solar energy, vol.153, pp. 64-76, 2017.

[8] M. Salimi, "Practical implementation of the lyapunov based nonlinear controller in DC-DC boost converter for MPPT of the PV Systems", Solar Energy, vol. 173, pp. 246-255, 2018.

[9] M. Rezkallah, S.K. Sharma, A. Chandra, B. Singh, D.R. Rousse, "Lyapunov function and sliding mode control approach for the solar-PV grid interface system", IEEE Transactions on Indust. Elect., vol. 64, pp. 785-795, 2017.

[10] M. Vatani, M. Hovd, "Lyapunov-based proportional-integral controller design with guaranteed region of convergence for dc-dc power converters", 12th IEEE Conf. on Indust. Elect. And Aplications (ICIEA), vol. 17, No. 7, June 2017.

[11] S. Fahad, N. Ullah, A.J. Mahdi, A. Ibeas, A. Goudarzi, "An advanced two-stage grid connected PV system: A Fractional-Order Controller", International Journal of Renewable Energy Research-IJRER, vol. 9, No. 1, pp. 504-514, 2019.

[12] I. Kocaarslan, S. Kart, N. Genc, H. Uzmus, "Design and application of PEM fuel cell-based cascade boost converter", Electrical Engineering, vol. 101, pp. 1323-1332, 2019.

[13] S. Kart, H. Uzmus, N. Genc, "Modelling and simulation of extremum seeking control for PEMFC", IJTPE Journal, vol. 9, No. 4, pp. 21-25, 2017.

[14] J.C. Amphlett, R.M. Baumert, R.F. Mann, B.A. Peppley, , Roberge, R.R., Harris, T. J. , "Performance modelling of the Ballard IV solid polymer electrolyte fuel cell", Journal of Electrochemical Society, vol. 142, pp. 9-15, 1995.

[15] P. Ahmadi, I. Dincer, "Exergoenvironmental analysis and optimization of a cogeneration plant system using multi model genetic algorithm (MGA)", Energy, vol. 35, pp. 5161-5172, 2010.

[16] M. Demirtas, I. Sefa, E. Irmak, I. Colak, "Microcontroller based DC/DC boost converter for solar energy systems", Journal of the Faculty of Engineering and Architecture of Gazi University, vol. 23, No. 3, pp.719-728, 2008.

[17] N. Genc, Y. Koc, "Experimental verification of an improved soft-switching cascadeboost converter". Electric Power Systems Research, vol. 149, pp. 1-9, 2017.

[18] A. Mamizadeh, N. Genc, and R. Rajabioun, "Optimal Tuning of PI Controller for Boost DC-DC Converters Based on Cuckoo Optimization Algorithm", 7th International Conference on Renewable Energy Research and Applications (ICRERA), Paris, 14-17 oct, 2018.

[19] N. Genc, I. Iskender, "Steady state analysis of a novel ZVT interleaved boost converter", International Journal of Circuit Theory and Applications, vol. 39, pp. 1007-1021, 2011.